# *Chapter V*

**CHAPTER-V**

# GAS SENSING PROPERTIES OF PURE & DOPED COBALT OXIDE NANOPARTICLES

## 5.1. Introduction

In current years, sensors used to detect various types of gases are highly enhanced. Hazardous or horrific gaseous & odours are often experienced in the environment, for long time gas sensors aimed at $NH_3$ that are used in industries [1]. Sensing of the variety of gaseous produced from food industries had emerged highly which frequently exists in small proportions in combination with countless harmful gases. The current international problems of energy and pollution in the environment necessitate the invention of detectors sensing $SO_X$, $CO_X$ & $NO_X$ in the environment or can be utilized to manipulate the structures of ignition drains from automobiles & industries.

Several sensors are implemented for targeting new gases. Additionally, unique sensor is required for identical gases relying on stipulations for sensing. Necessity for sensors to detect the extent of air pollution is increased. Thus required measures are taken to manage pollution. Additionally, monitoring hazardous gases is required for guard against unwanted incidence of fire or explosion. Density of these gaseous in environment have to be measured in parts per million. Though many gases (for instance $H_2$) lose their toxicity at the ppm stages, they are inflammable in certain explosive combinations while their percentage is above threshold value [2-4].

The requirements of the human race had increased greatly due to industrial revolution in previous few years. Technological innovations to meet these demands have added a good number of environmental pollutions. Industrialization growth & increasing exhausts by vehicles have accelerated air pollution. In this scenario, detecting hazardous, toxic & flammable gases are essential for protecting environment.

Important element in various methods regulates, output enhancement, atmosphere observation & so on is size of attenuation for different gases issues of surroundings. Hence conditions worthy sensors could furnish integral interface connecting ambient & backup digital instruments for observing particular gas. So that sensors for rapid detection of poisonous & inflammable chemical compounds are required.

A gas sensor is defined with an aid of the International Union of Pure and Applied Chemistry (lUPAC), "a chemical sensor is a device that transforms chemical information, ranging from the concentration of a specific sample component to total the composition analysis, into an analytically useful signal. The chemical information mentioned above may originate from a chemical reaction of the analyte or from a physical property of the system investigated"[5].

Receptor & transducer are the 2 most important elements encompassed by chemical sensors. Receptor converts chemical information to energy that is measured by the usage of the transducer. The transducer transfer energy usually to electrical & analytical signal.

According to Stetter & Penrose, characteristics of chemical sensors [6] are:

- The Sensitive layer is chemically contacted by analyte
- While sensitive layer is exposed to analyte change in reaction occurs.
- Transduction of charge to electric signals is allowed in sensitive layer.
- They have small structure.
- They are real time operators.
- They won't automatically measure a signal
- Usually they are affordable & reliable.

**5.2. Classification of Gas Sensor**

On the basis of employed strategies, chemical sensors are categorized & it depends on receptor's operating principle [7]. Utilizing this precept, physical, chemical & biochemical sensors are distinguished. The absence of chemical reaction at receptor occurs in physical sensors & signal is the end result of structural procedures, which include changes in absorbance, mass, temperature, refractive index/ conductivity exchange. Chemical reactions among analyte molecules & receptor are the basis of chemical reactions [8-12]. Biochemical reactions are done in biochemical sensors which is a subclass of chemical sensors.

### 5.3 Characteristics of Gas Sensors

The parameters used to characterize sensor performance are listed below [13-17].

- Change in measured signal per analyte concentration unit is Sensitivity which is confused with detection limit. It is the slope of calibration graph.
- The ability of a sensor to determine selectively to a single or group of analytes is referred as selectivity.
- Capability of sensor to give repeated results after specific duration is named as stability. It involves retaining sensitivity, selectivity, response & recovery time.
- At a specific temperature & provided conditions, the least amount of analyte detected by a sensor is termed as Detection limit.
- Dynamic range is an analyte concentration range among detection limit & highest concentration limit.
- Relative deviation of calibration graph from ideal straight line is the linearity.
- Least concentration gap identified by sensor is Resolution.
- The response time is the duration of time taken by sensor to achieve 90% of the maximum value in every measurement.
- Recovery time is the time required for sensor signal to back to their initial value before introducing gas in every measurement.
- Temperature at which maximum sensitivity is achieved is referred as working temperature.
- Highest variance in result achieved while having increased & decreased range of analyte concentration is Hysteresis.
- The time taken for a sensor to operate continuously is termed as life cycle.

An ideal chemical sensor should achieve higher sensitivity, dynamic range, selectivity, stability, less detection limit, better linearity, low hysteresis, response time & lengthy life cycle. Commonly scientists try to achieve only some of these ideal properties by eliminating others. Because generating an ideal sensor is a tough job. Generally for

real applications all the properties are not required. In atmospheric applications, while quantity of pollutants change gradually, need of detection limit is greater, yet response time of a fewer minutes is admissible.

The various reason for gas sensor's instability are design errors, structural changes, phase shifts, poisoning initiated by chemical reactions, changes in environment. These problems can be solved by utilizing substances having chemical & thermal stability, regulating elemental composition & grain size of sensing materials, using particular technologies for surface pretreatment of sensors.

### 5.4. Previous Investigation

Electrical resistance of semiconductor is highly sensitive to impurities in its surface. It was experimented for Ge in 1953 [19]. Then conductivity of ZnO thin films heated to 300°C is sensitive reactive gases in environment [20]. For $SnO_2$, comparable features were reported with higher stability [21]. Furthermore enhancement of commercial gas sensors was developed by those results.

Initially metal oxide sensors hold many unsatisfactory properties like prominent cross-sensitivity, sensitivity into humidity, lengthy signal drift & gradual sensor response. For improving sensor performance, numerous metal-oxide semiconductors are experimented [22]. Trial & error method was employed in initial stages as the sensor response mechanisms were not clearly understood.

Recently, concern on gas sensitive materials improved distinctly for development in nanotechnology. It is connected to electronic properties of nanomaterials like size dependence & capability for controlling material structure through modern experimental techniques [23]. Many substances & devices were improved yearly through nanotechnology [24-26].

Mostly p-type oxide semiconductors like NiO, CuO, $Co_3O_4$, $Cr_2O_3$, & $Mn_3O_4$ of transition metals show different oxidation states due to electrons in d shell of metal atom [27]. Usually they exhibit diverse catalytic activities which enhance oxidation of volatile organic compounds like CO, $NH_3$, $C_2H_6$, $CH_3CHO$ since p-type oxides exhibit attraction with oxygen & multivalent properties [28-38]. Hence, P-type oxides offer a committed

base for improving highly executing gas sensors. It is noteworthy that the Detecting ammonia gas is remarkably a difficult job by p-type oxide gas sensors, were attained by synergetic bond of p-type sensing (Co-O) & n-type dopant (Fe-O) substances by different catalytic properties with a high degree of sensitivity.

### 5.5. Present study

Gas sensitivity of pure cobalt oxide was experimented & correlated with n-type and p-type dopants that of Zn, Fe, Cu and Ni doped cobalt oxide nanoparticles. From the obtained results, it has been proved that the Fe doped cobalt oxide nanoparticles are more efficient than those obtained with the other three dopants. In many cases, sensitivity plays a vital indicator in the framework & application of sensors. When the quantity of toxic gases is increased in the atmosphere, before reaching the threshold value sensors must provide adequate signals to people.

### 5.6. Introduction to Sensing Set up

This section gives a detailed account of gas sensing materials protocols adopted for the synthesis of temperature independent in first part. A detailed description of sensor fabrication techniques used for this investigation and the evaluation of gas detecting characteristics of developed materials are given.

### 5.7. Factors Influencing the Sensitivity

Addition of dopants on metal oxide gas sensors could enhance the sensitivity. It can direct towards the production of new donor/acceptor energy states that changes grain size & growth mechanism [39]. Firstly, reduction of gas molecules is activated through creating active surface species which react by spillover method by charged oxygen molecules adsorbed on metal oxide. It can direct the reinjection of localized electrons or holes return to the matter by increasing/decreasing conductivity of material.

Different semiconductor oxides will differ in thickness between 1-100 nm. Researchers explained that sensitivity increases with decrease in grain size & low specific surface area [40-48].

Temperature dependence of metal oxide sensor signal appears for various causes. Firstly, charge of the oxygen species absorbed at surface depends on temperature [49].

Secondly, rate of oxidation reaction increases with temperature. Lastly, process that depends on temperature are adsorption, desorption & diffusion [50]. Variation in temperature directs to response graph due to the properties of particles in gas mixture [51].

### 5.8. Structure of Sensing Layer

Metal oxide gas sensor comprises of various components: sensitive layer, substrate, electrodes & heater. Using screen printing on small & thin ceramic substrates metal oxide gas sensors was synthesized. By this method, thick films of metal oxide semiconductor may accumulate into batch processing that led to variation in properties of various sensor components. Alumina, LTCC (low temperature cofired ceramics), silicon technology are commonly used as gas sensor substrates.

However, Implementation of manufacturing process attains several demerits. Firstly, difficulty in keeping thick metal oxide film at higher temperature as a result power consumption of screen-printed sensors are higher as 1W [52], so it can be utilized in battery used devices. Next drawback is the appropriate mounting of overall hot ceramic plate in order for better thermal isolation of sensor component & housing. Due to these drawbacks, researchers promoted the synthesizing of sensitive layer.

A promising solution is to integrate sensing layer using microelectronic manufacturing that overcomes barriers of screen-printed sensors. Here oxide layer is coated on thin dielectric membrane having lower thermal conductivity that gives better thermal isolation of substrate from heated area on membrane. It leads to low power consumption. However, total size of single sensor elements are decreased then minimum gap of electrodes in μm is obtained. Combination of signal-processing electronic elements & substrate having multiple sensor components are achieved.

### 5.9. Methods of Measurement

By calculating resistance/conductance of sensor component in air & certain concentration of analyte gas can be used for testing response. Response of sensor can be detected by flow through method & static environment method [53].

### 5.9.1 Flow Through Method

Here, response curve detected using a constant flow of analyte gas. Quantity of analyte gas is maintained through combining that to a carrier gas by mass flow controllers (MFC). MFC is switched off to obtain recovery measurements.

### 5.9.2 Static Environment Method

Sensor element of certain volume is mounted in a closed chamber. Specific concentration of gas is injected through a syringe to measure the sensor resistance until a constant state is attained. Through ejecting sensor from housing & exposing to air, recovery of sensor is examined.

## 5.10. Drop coating of sensing materials

Method of film processing is categorized into two: thin-film deposition methods for thicknesses between 0.005-2 μm, like sputtering, evaporation & chemical vapor deposition. For thicknesses larger than 10 μm, thick-film deposition methods like screen printing, drop coating & tape casting are used. Above ~50 μm thickness, thermal spraying is utilized for attain coatings of metals, ceramics & cermets.

In this study, drop coating method is exploited for preparing gas sensor films [54]. Drop coating is simple, easier & faster method widely used for surface preparation for chemically developed electrodes that altered layer consists of nanoparticles used for electrocatalysis for chemical sensing and materials evaluation. In this method, a mixture of required metal oxide powder by an appropriate solvent is coated on a substrate commonly using regulated injection by a pipette. In order to enhance adherence to substrate the coated layer is heated to avoid solvent [55]. Film microstructure & sensor performance depends upon configuration of mixture & nature of dropping [56]. By changing number of deposited drops specific thickness are achieved & it depends on solution's viscosity. A quantity of 1 mg material is dispersed in 1 ml ethanol. Solvent gets evaporated by itself/heating, after the deposition of solution.

## 5.11. Electrical Characterization

By the use of Keithely 195A digital multimeter electrical properties of metal oxide sensors were achieved by examining D.C. resistance of specimen before & after injecting gas. Sensitivity for oxidizing & reducing gas is represented as the ratio $R_{gas} / R$

$_{air}$ & R $_{air}$ / R $_{gas}$ respectively. By connecting a load resistance ($R_L$) in series with sensor resistance ($R_S$) is another way to measure sensor resistance [57-59]. To achieve current $I_S$ a voltage ($V_c$) is supplied to the connection of $V_S$ & $V_L$ that drops voltages across sensor & load respectively. Sensor resistance is measured by calculating the output voltage across the load & also current beside sensor while constant dc voltage is supplied [60, 61]. By measuring the change in dielectric constant of films between electrodes are done in gas sensors of capacitive type like a function of gas quantity. Capacitance depends on operating frequency & environment such as humidity & temperature. Capacitive sensor depends on inter digitated electrode structures that has two plates of a standard capacitor for monitoring variations of dielectric coefficient of film.

Sensor characterization is significant for ensuring the functions of gas sensor for optimizing their use due to its complex mechanisms. Various performance tests on the basis of parameters are needed for all sensors to be marketed.

### 5.12. Fabrication of gas sensor device

Photograph of gas sensing setup is shown in Fig. 5.1. In the test system, a test chamber for the purpose of measuring gas sensor is incorporated with facilities for both static and dynamic measurements. The static method of measurements has been employed, and volume ratio determines the gas concentration. Temperature controller brings the sensor to desired temperature. When desired temperature reaches adequate amount of gas is given to pre calibrated gas cylinders by a syringe & injected to test chamber. Change in sensor resistance in the existence of test gas is monitored through a Keithley 195A digital multimeter at atmospheric pressure. Test system composed of a stainless steel chamber of 280 ml volume, 7.5 cm diameter & height 6.35 cm. For introducing adequate amount of test gas through an inlet with a septum into a chamber using a syringe. For purpose of exhaust purpose a valve is connected at the outlet of chamber. Dynamic calculations are done by connecting this valve to inlet of a vacuum pump. Using silver paint 2 thin copper wires are connected to sensor as electrical connections. Sensing abilities of sensor are characterized at various operating temperatures to precise optimum temperature. Inside the chamber, a heater (nichrome wire wound around mica sheet & inserted between two copper pieces) is used to heat the sample at required temperature.

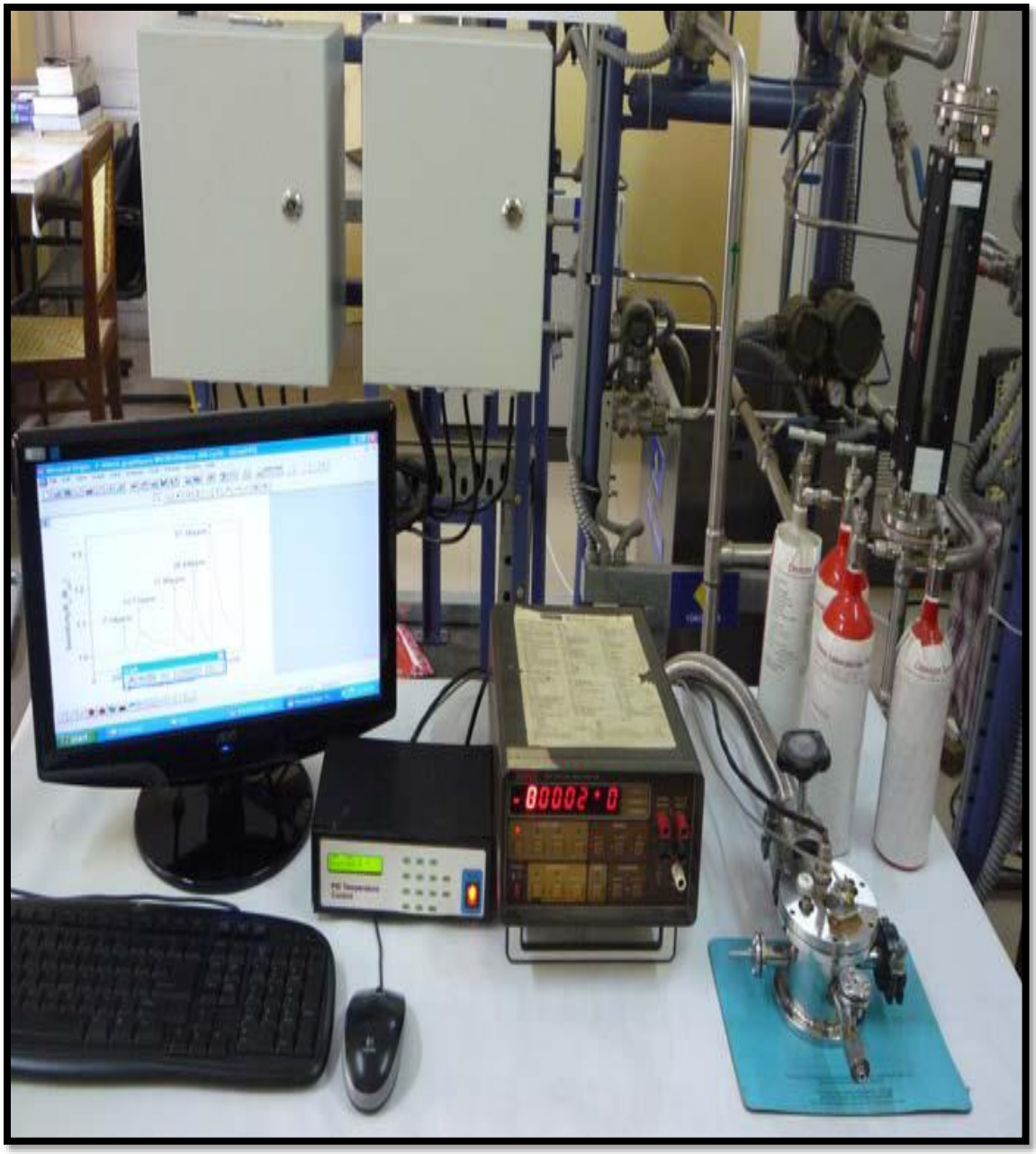


**Figure 5.1. Gas sensing setup**

## 5.13. Fabrication of Interdigitated Array Electrode (IDA) using DC Magnetron Sputtering

Gas sensing performance was measured by an interdigitated array (IDA) electrode of Au thin films on alumina substrates. The Inter digitated Array Electrode was manufactured by DC magnetron sputtering of gold. Fabrication of the inter digitated array (IDA) electrodes on $Al_2O_3$ substrate (99.6% purity) was carried out using a shadow mask by DC magnetron sputtering. Gold coated IDA sensing electrodes on alumina substrates were used for temperature dependent electrical conductivity measurements & gas sensing studies. Fig. 5.2a exhibits Auto CAD design of IDA and Fig.5.2b shows the fabricated IDA mask. DC magnetron sputtering technique was used to prepare the IDA electrode using shadow mask. Distance between two inter digitated electrode fingers was 50 μm and width of each electrode was 0.5 mm. Thin films of the sensing materials were spin coated onto the IDA electrodes.

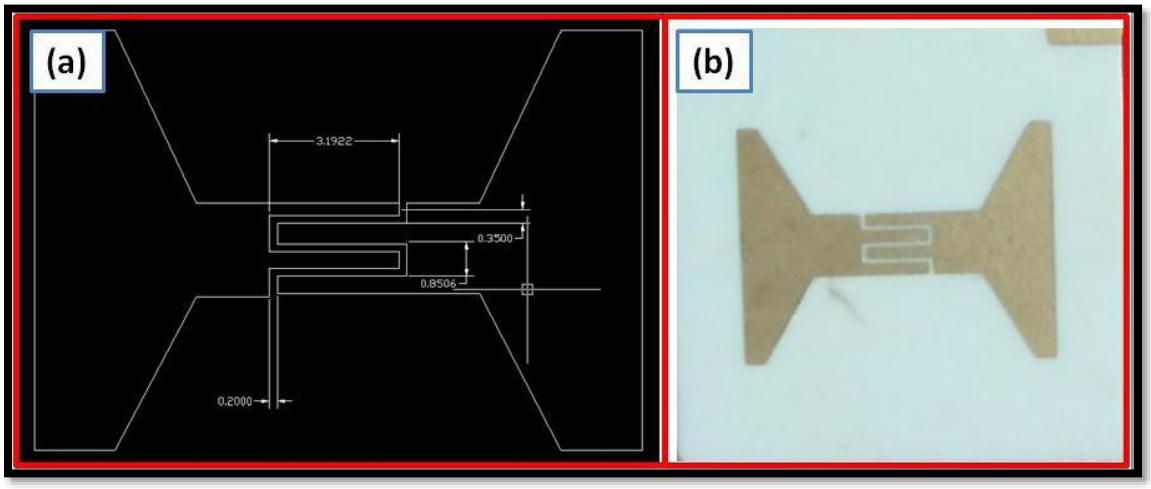


**Figure 5.2(a) AutoCAD design of IDA mask and (b) fabricated IDA mask.**

Fig.5.3. shows the photograph of the DC magnetron sputtering unit used for fabrication of the transducer electrodes for the sensor. The principle of the coating includes attacking the donor material by ionized gas molecules driven by high applied potential at low pressure. Emission of atoms from target resulted because momentum transfers between the incident ions and the target. These high energy atoms adhere to the recipient material at the anode & form a thin film on its surface.


**Figure: 5.3. Photograph of DC magnetron sputtering unit for fabricating IDA electrodes**

For this investigation, a 2” diameter circular gold disc was used as the target for sputtering. The whole chamber was grounded and the system is attached to a diffusion pump backed with a rotary pump for creating vacuum. During coating, the target was fixed at the cathode, the substrate with mask was kept at the anode (ground) and a

working pressure in the range of 10-3 mbar was maintained with argon flow. Voltage of ~1000V was applied for sputtering. The Ar ion in plasma is accelerated toward the cathode, hits the target and transfers the energy for sputtering gold atoms that deposit onto the substrate surface. Typically, gold electrode of 200 nm thickness and dimensions corresponding to the window present in the shadow mask was coated in 3 min. Alumina was used as the substrate upon which the Gold IDA electrode was fabricated. The sensor materials were coated by spin coating technique for evaluation of sensor properties.

### 5.14. Electrical conductivity measurement set up of the sensor

The electrical conductivity measurements of synthesized $Co_3O_4$ on the basis of sensor materials were performed using electrometer (Keithely Instruments, model-SMU-2420, USA) at room temperature under ambient conditions (Fig. 5.4). Electrical resistance were carried out using a Linkam probe station (Linkam's THMS600, Finland) with controlled heating or cooling rates (10°C/minutes) and high level accuracy and stability. The Linkam probe station operates temperature between -196°C - 600°C with a temperature sensitivity < ±0.1°C. A silver heating block aids high thermal conductivity. Direct injection of coolant to silver block is also facilitated.

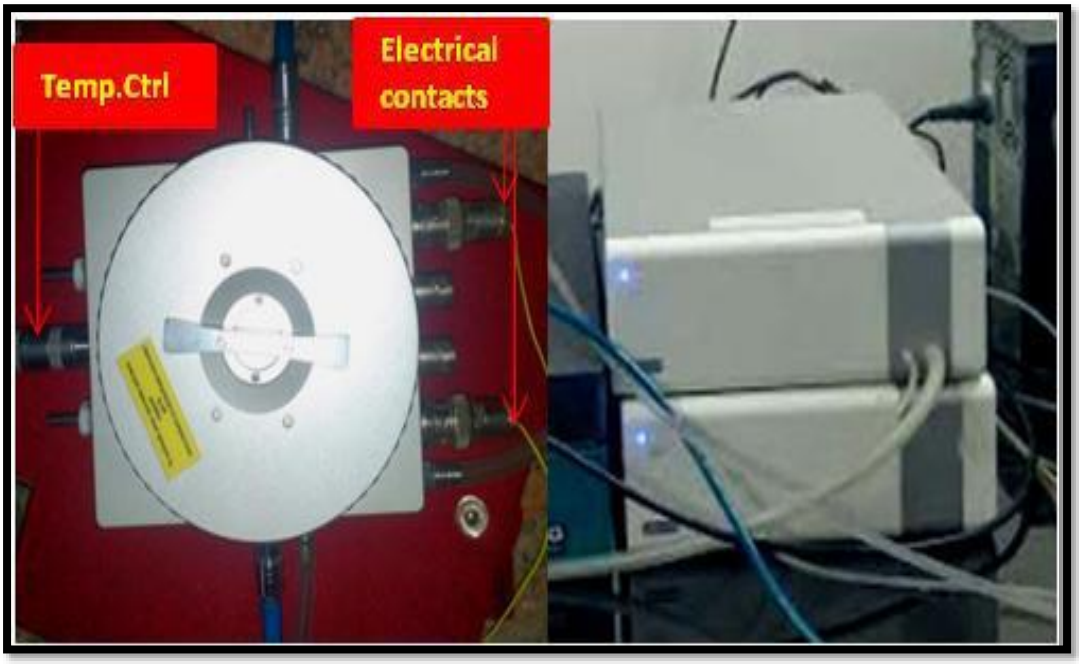


**Figure: 5.4. Photograph of Linkam probe station used for temperature dependent electrical properties of sensing materials**

### 5.15. Experimentation and Determination of Gas Sensing Properties

A custom built gas senor test station is used for analyzing gas sensing characteristics were developed at Nanosensor Laboratory, PSG Institute of Advanced Studies, Coimbatore (Fig. 5.5). The facility consisted of a modified stainless steel twin vacuum chamber, the first for mixing the gases and the second for testing. It is equipped with a proportional integral derivative (PID) controlled heating stage and tungsten probes for electrical measurements. The chamber is composed of a double wall stainless steel gas assembly unit, *in-situ* heater stage, electrical connections and computer interface for monitoring sensor signal using Keithley sourcemeter 2420 (U.S.A.) joined by data acquisition system using LabVIEW software. In this setup, the fabricated sensor was connected with electrical wires using silver paste and carefully loaded into the Sensing Set up (SS) gas chamber. While measuring the test gas is added by nitrogen (N2) to attain required quantity & the flow rate is regulated at 100 sccm by Aalborg MFCs (U.S.A.). An Eurotherm (2420) temperature controller (U.K.) is utilized for regulating working temperature of electrode substrate inside sensing chamber. Gas delivery system connected with SS twin chamber was suitably modified to send the gas mixture with the required ppm level of analyte gas.

The gas mixing scheme is shown in Fig. 5.5. The analyte gas was mixed in two stages; the oxygen gas (MFC-1) is mixed with carrier gas (MFC-2) and stored in Mixer-1. A specific amount of the mixed gas from the Mixer is sent through a third MFC and was further diluted by carrier gas from the first MFC, such that one can get the required ppm level of oxygen in carrier gas in two stages. This scheme can be extended further to dilute the oxygen to achieve the desired ppm level of oxygen. All MFCs are connected with one way valves to avoid back flow of gases. Further, in order to achieve the specified mixing ratio, the MFCs were always maintained at positive pressure between the gas inlet and outlet. An Agilent Multimeter 34410A was used for measuring the electrical signal from the sensors.

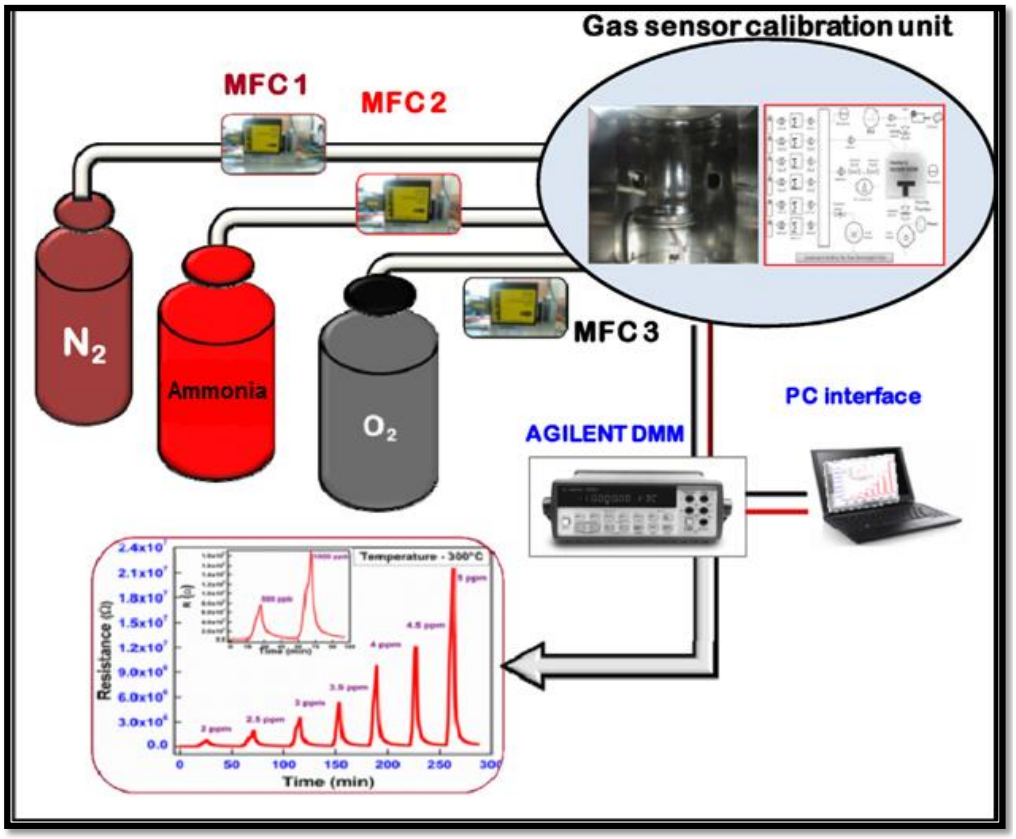


**Figure: 5.5. Custom-built gas sensor test station facility at PSGIAS used for sensing analysis**

A custom built gas sensor is used for gas sensing studies. Gas sensing characteristics are carried out by WS-30A designing frame (Winsen Electronics Co. Ltd.) below static conditions utilizing gas sensor like a stainless steel double walled test chamber by a temperature controlled hot level sensor holder, mass flow controllers (MFC, Aalborg, U.S.) & Keithley supply meter (2420, America), connected using data acquisition device by Lab VIEW software. While $NH_3$ gas is mixed by dry air for achieving required quantity& flow rate maintained at 200 sccm through mass flow controllers (Aalborg, united states A.). A temperature controller (**EUROTHERM, 2420, U**. K) was utilized to manage the working temperature of the sensor implemented in sensing chamber. Humidity measurement was skilled by a gas generator (Owlstone OHG-4 humidity generator). The sensor response (S) is executed by measuring the change in electrical resistances of sensor in air ($R_a$) & target gas ($R_g$) [62].

### 5.16. Gas Sensing Properties of Cobalt oxide Nanoparticles

The $Co_3O_4$ nanopareticles exhibited a gas-sensing at surface of sensor material. Response of sensor is enhanced gradually by increase in gas concentration that is graphed in Fig 6. Typically a p-type semiconductor increases resistance with amount of reducing gas. Decrease in resistance occurs in an n-type [63].

When a gas reaches the sensor, it is detected through a chemical reaction. While $NH_3$ is syringed & steady at certain concentration then resistance will increase suddenly & falls abruptly behind the withdrawing of $NH_3$. These actions are recycled by various gas concentrations like 1ppm, 2ppm, 3ppm, 4ppm and 5ppm.

Fig. 5.6 (a) shows the variation of sensitivity of cobalt oxide sensor at room temperature with concentration varying from 1ppm-5 ppm. The sensitivity is maximum at a 5 ppm concentration, below which sensitivity reduces. Response & recovery time of the sensor for a concentration of 5 ppm gas at room temperature are revealed in Fig 5.6 (b). Comparitively small values of 30 & 51 seconds are achieved as response & recovery times respectively. An increased sensitivity of 5.6 was attained for 5 ppm at room temperature.

These results exhibited that sensor was capable of determining sensitivity of 3.6 at low concentrations of 1 ppm. I-V analysis indicates that the sensor current decreased after the adsorption of the gas molecules. After gas adsorption, band gap energy changes & affects conductivity of material and increases channel resistance. The I-V operating point is responsible for gas response & signal drift. I-V curves were modulated at 1000 ppm and are shown in Fig. 5.6 (c). The linear fit measurements were performed and the regression coefficient $R^2$ was found to be 0.9965 (Fig. 5.6 (d)).

From present study, surface area & spherical structure of $Co_3O_4$ nanoparticles play a significant part in detecting the ammonia gas. For chemical/physical interactions number of active sites on surface is increased due to increased surface area. Samples having porous metal oxide architecture with large surface area & pore volume assured as a promising sensor materials.

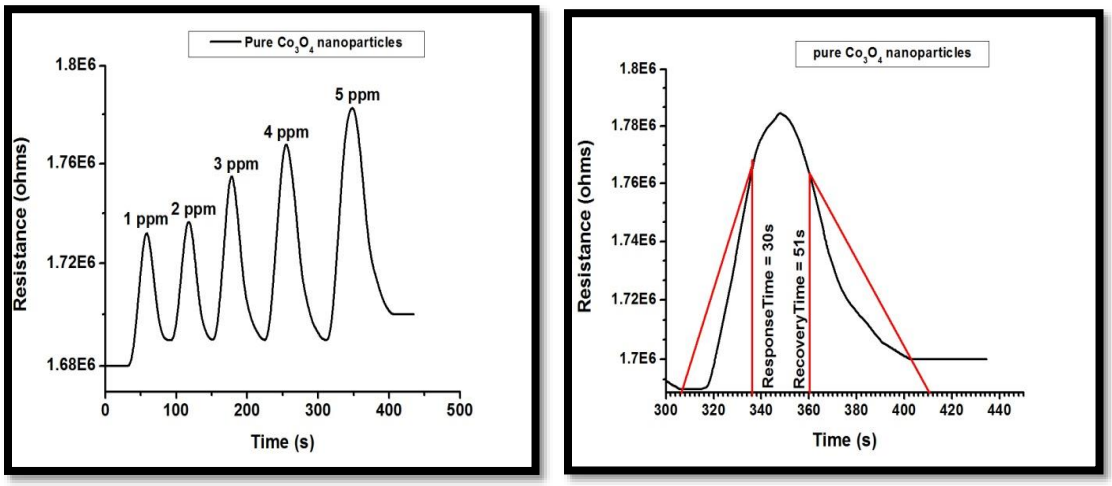


**Figure: 5.6 (a) shows sensitivity of pure $Co_3O_4$ nanoparticles at room temperature towards different gas concentration and (b) response and recovery time towards 5 ppm of $NH_3$**

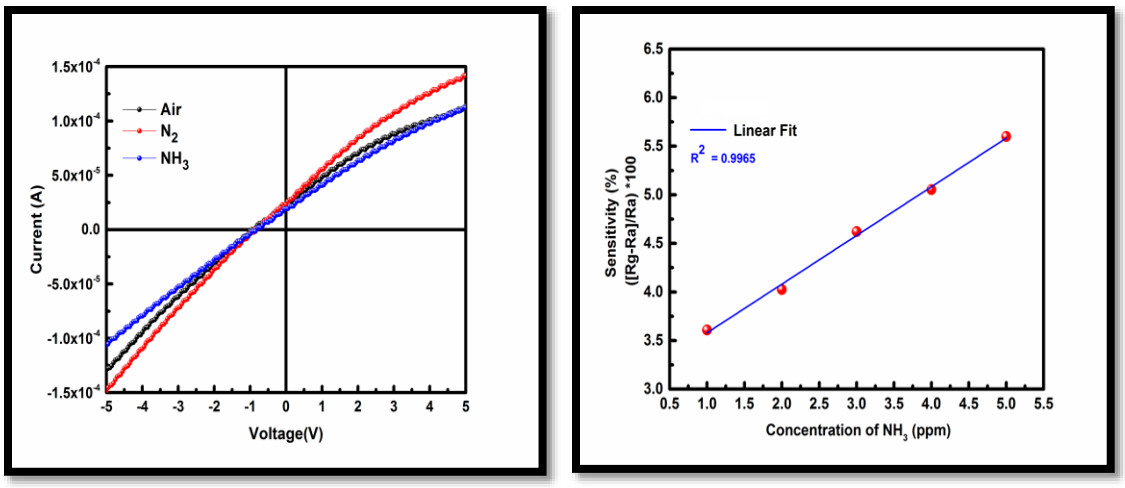


**Figure: 5.6 (c) I-V characteristics and (d) Sensor response linear fit plot of pure $Co_3O_4$ nanoparticles to $NH_3$ (1-5 ppm) gas at room temperature**

### 5.17. Gas Sensing Properties of Zn doped Cobalt oxide Nanoparticles

In Fig. 5.7 (a) variation of sensor sensitivity at room temperature with concentration (1-5 ppm) was shown. At 5 ppm concentration, the sensor showed maximum sensitivity of 8.9 below which the sensitivity decreases 4.4 at 1 ppm. Fig. 5.7 (b) shows the response and recovery times of the sensor at 5 ppm concentration. Response & recovery times were relatively small with values 14 and 38 seconds respectively. The excellent linear response suggests availability of many active sites. Creation of built-in potential beside p-n junction is due to asymmetric I–V features. When sensor is exhibited to analyte gas then change in quantity of current created underneath forward/reverse bias is utilized as sensor signal (Fig. 5.7 (c)). The sensor response value increased linearly on increasing the $NH_3$ concentration (1-5 ppm) with a regression co-efficient ($R^2$) of 0.9495 (Fig. 5.7 (d)).

The detection principle of sensor is the chemisorption of analyte gas through semiconductor metal oxide. Increased surface resistance of sensor is due to the action of the chemisorbed oxygen species as surface acceptors, catching electrons. When $NH_3$ gas is injected, it is responded by the creation of oxygen ions that emits the trapped electrons to sensor surface by a decrease in sensor resistance. This demonstrates that synthesized material is a p-type semiconductor [64]. Lone pair of $NH_3$ electrons plays electron donor to metal oxide by reaction having adsorbed oxygen ions on surface by restoring trapped electrons. Equation of this reaction is [65]:

$$2NH_3 + 3O^-_{(adsorbed)} \rightarrow N_2 + 3H_2O + 3e^-$$

In thermodynamics, electrons move from conduction band of $Co_3O_4$ to that of ZnO, but holes would locate reversely from valence band of ZnO to that of $Co_3O_4$ [66]. A p-n heterojunction is formed due to the electron-hole pair arrangement of $Co_3O_4$/ZnO & it led to higher resistance [67]. Higher sensitivity is assigned to electronic sensitization worked by $Co_3O_4$ [68]. Number of active sites of chemisorbed oxygen species on the surface of p-type is greater than on n-type semiconductors [69].

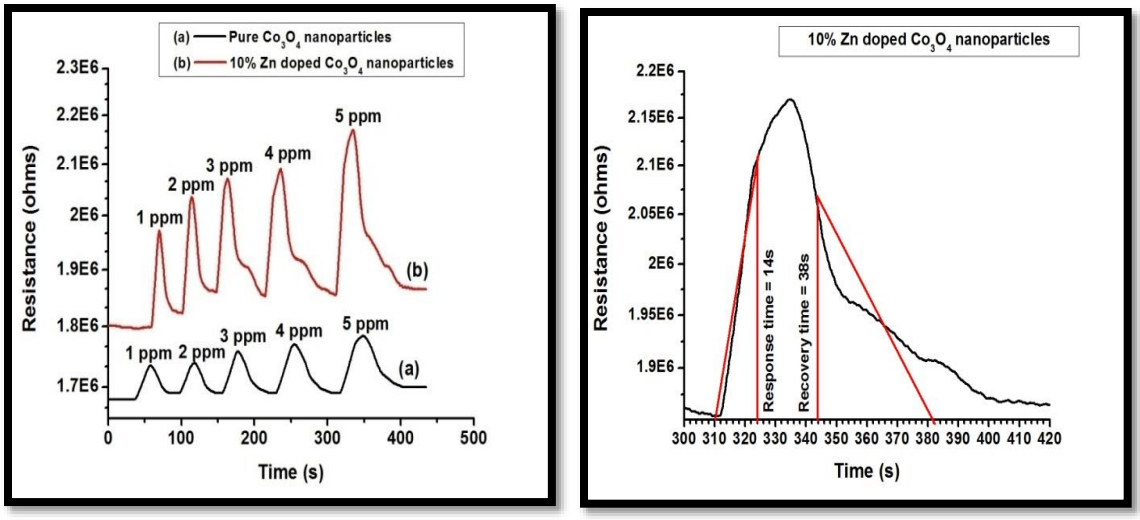


**Figure: 5.7 (a) shows sensitivity of pure and Zn doped $Co_3O_4$ nanoparticles at room temperature towards different gas concentration and (b) response and recovery time towards 5 ppm of $NH_3$**

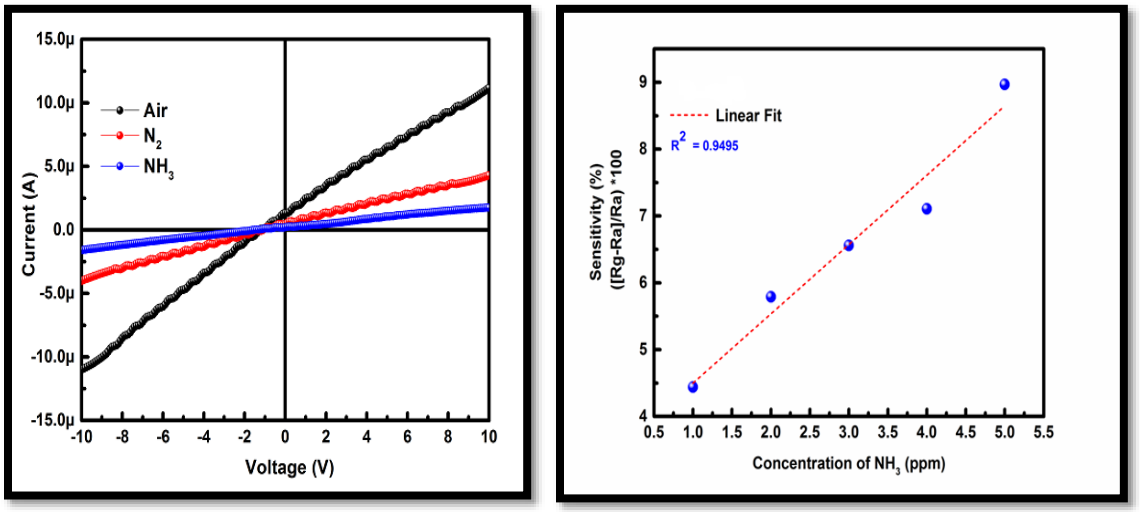


**Figure: 5.7 (c) I-V characteristics and (d) Sensor response linear fit plot of pure and Zn doped $Co_3O_4$ nanoparticles to $NH_3$ (1-5 ppm) gas at room temperature**

Charge transfer between the Fermi energy levels of ZnO & $Co_3O_4$ is occured. Electrons from $Co_3O_4$ are caught by oxygen molecule in the air & are accumulated on their surface [70]. Meanwhile, an electron depletion layer is formed due to the motion of electrons from ZnO to $Co_3O_4$ & triggers conductivity process & lead to empower sensitivity of ZnO doped $Co_3O_4$ nanoparticles [71,72].

By using $R_a$ & $R_g$, estimating response calculation is difficult. Change in resistance is decided by the semiconductor type& target gas [73].The performance $NH_3$ gas sensor, is based on $R=R_a/R_g$ condition where $R_a$ & $R_g$ are resistances of sensor in air & target gas respectively. [74].

In Fig.6 Sensor response for both pure & Zn doped $Co_3O_4$ nanoparticles towards 1 - 5 ppm of $NH_3$ is shown. Response of sensor & gas concentration is directly proportional [75]. Zn doped $Co_3O_4$ nanoparticles show significant sensitivity toward $NH_3$ gas [76,77]. The gas concentration is directly proportional to change in resistance. It is based on dynamic equilibrium among $NH_3$ adsorption & desorption process on surface of ZnO [78, 79]. At the time of adsorption of oxygen species on surface of ZnO electron capture is occurred [80, 81]. While Zn doped $Co_3O_4$ surface is revealed to $NH_3$, response to $NH_3$ gas enhances due to the movement of much electrons back to conduction band of ZnO [82-84]. Better gas response is attained for higher concentrations & it is assigned to availability of numerous analyte molecules intersecting by active sites at the gas exposure time [85, 86]. These results revealed 2 important properties like it reduce working temperature of sensor & it improves sensitivity towards ammonia gas concentration [87, 88].

To improve space charge region through doping of oxide-oxide p-n junctions is an affordable & reliable technique for enhancing response of MOS toward gases. In Zinc doped $Co_3O_4$ material revealed higher response to $NH_3$ at room temperature of 5 ppm gas concentration for various applications [89-91].

Electronic conductivity changes through the association of imperfections inside nanoparticles are basis of doping. Sensitivity of nanoparticles sensors enhances due to these variations. Change in conductivity can vary Fermi level in energy band diagram that alters transfer of electrons among gas molecules & nanoparticle material [92-94].

Dislocations of free charge carriers are the significant process that reverses effect of adsorbed analytics. The merits of low temperature, better crystal quality, rapid & simple fabrication & high performance had made Zn doped $Co_3O_4$ nanoparticles as an efficent gas sensor material. Higher mobility of conduction electrons made ZnO a promising candidate for gas sensors. Commonly, n-type nanoparticles had higher operating temperatures than p-types so that Zn doped $Co_3O_4$ nanoparticles were prepared & its sensitivity increased due to the decrease in grain size through adding of 10% ZnO.

### 5.18. Gas Sensing Properties of Fe doped Cobalt oxide Nanoparticles

Selective detection for gases by iron oxide nanoparticles (IONP) is due to change in bandgaps, atomic fractions & exhibited crystalline faces in crystallographic manners [95]. While nanosized IONP structures absorb gases, resistivity is varied that detects proportional variation in current [96,97]. Decrease in hole concentration due to dopants makes chemiresistive changes because of electronic sensitization that improve gas response of Fe doped $Co_3O_4$ nanoparticles [98]. Different conduction properties are revealed by adsorbing oxygen on electrical layers in metal oxide semiconductors. Sensor resistance of n-type semiconductors is examined through resistive contacts created among particles in oxide semiconductors. However, equal circuits of n-type semiconductor gas sensors are described as serial connections among semiconducting cores ($R_{core}$) & resistive inter particle contacts.

Sensor resistance is increased due to reduced hole concentration while electrons are released because of reaction between gas molecules & adsorbed oxygen [99]. When iron is inserted into $Co_3O_4$ then weakening of Co-O bond occurs due to the expansion of unit cell volume. The reducing of apparent activation energies by iron substitution results in rapid oxygen adsorption & desorption [100]. Tuning of charge carrier concentrations at certain operating temperature is used to attain higher responses to gases by controlling resistance of sensor to make the circuit simple. In p & n-type oxide semiconductors, majority of charge carriers at the surface & oxygen anions are different.

"Electronic sensitization" is the improvement in gas response through tuning of charge carrier concentration [101]. The earlier reports explained the utilization of doping [102, 103] for decreasing /increasing number of electrons in the semiconductor.

Through recombination reaction the substitution of Fe ions in Co sites decreases the concentration of holes in Co. It is the reason for increase in sensor resistance by increasing Fe dopant concentration. These findings suggested the correlation of gas response of the sensor and concentration of charge carriers in material. That is, comparing with undoped Co number of electrons injected into the sensor, is highly sensitive to Fe doped Co.

Cobalt oxide, is usually used to provide Oxygen Evolution Reaction (OER) active sites for stronger adsorption capability of oxygen ions. Likewise, enhanced OER activity is due to the inserting of Fe in cobalt oxide catalysts. Fe-doped $Co_3O_4$ creates active oxyhydroxide which differs from $Co_3O_4$ but Co ions are the reason for OER active sites & it enhances sensor efficiency.

Sensitivity of sensor towards concentration (1-5 ppm) at room temperature is shown in Fig. 5.8 (a). It is found that at 5 ppm the sensor has a maximum sensitivity percentage of 18.4. The lowest sensitivity of 6.5 was observed for the lowest concentration (1ppm). Response & recovery time of sensor for concentration of 5 ppm at room temperature is revealed in Fig. 5.8 (b). The sensor experienced 15 seconds for response time & 31 seconds for recovery time. I-V characteristics exhibited a change in current with decrease in adsorption of gas molecules. Due to change in energy band gap after the gas adsorption, the conductivity of the material is affected and there is an increase in the channel resistance. The linear fit measurements were performed and the regression coefficient $R^2$ was found to be 0.9552. The I-V characteristics and linearity curve are respectively exhibited on Fig. 5.8 (c) & (d).

By geometrical confinement & electronic interactions Fe changes characteristics of Co in $Co_3O_4$ lattice. The enhancing of OER activity is evident by introducing Fe ions to cobalt oxide lattice. However, properties that hold Co ions in lattice are utilized as active sites for OER is investigated. While a low concentration of Fe ions is inserted alters manner of active site. Reason for enhancement of OER activity may due to vary in electronic structure & rapid charge transfer rate by addition of Fe ions.

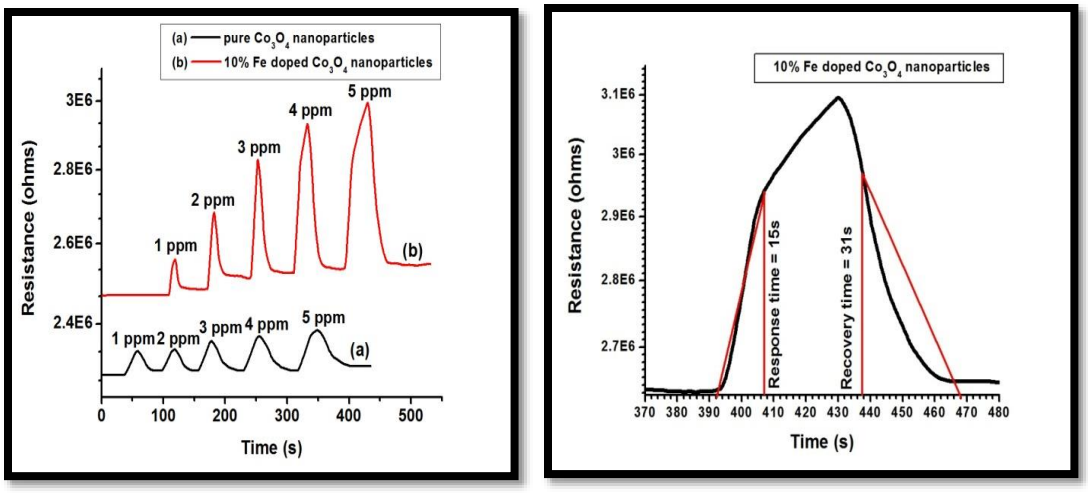


**Figure. 5.8 (a). Sensitivity of pure and Fe doped $Co_3O_4$ nanoparticles at room temperature towards different gas concentrations and (b) Response and recovery times for 5 ppm of $NH_3$**

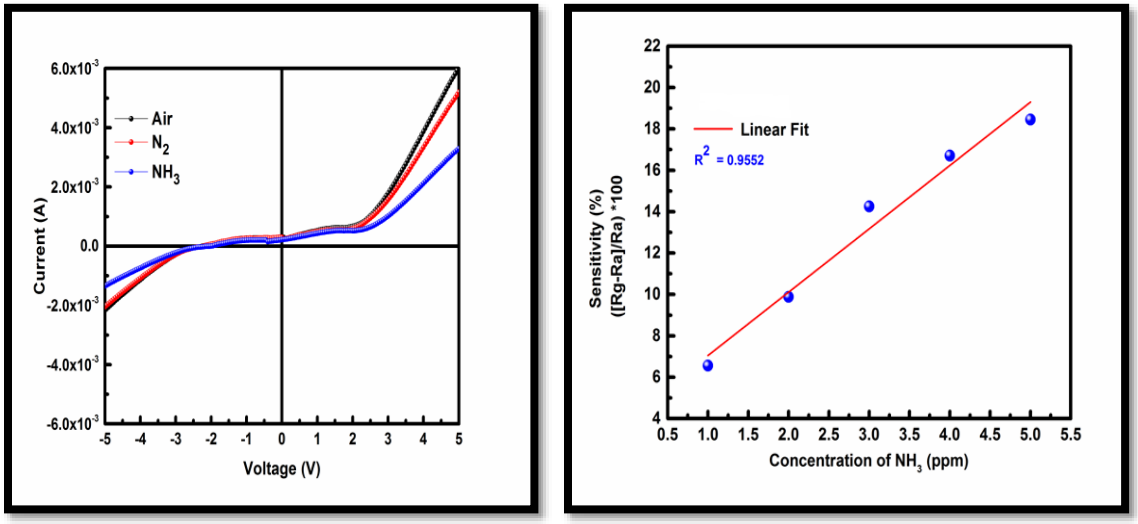


**Figure. 5.8 (c) I-V characteristics and (d) Sensor response linear fit plot of Fe doped $Co_3O_4$ nanoparticles to $NH_3$ (1-5 ppm) gas at room temperature**

$NH_3$ adsorption on the catalyst surface is enhanced by the optimization of Co ions on catalyst surface by introduction of Fe to $Co_3O_4$. Oxygen species on Fe doped $Co_3O_4$ is highly active than $Co_3O_4$, & while there occurs a lack of oxygen, in lattice oxygen of Fe doped $Co_3O_4$ can rapidly overflow to surface for participating in oxidation reaction.

### 5.19. Gas Sensing Properties of Cu doped Cobalt oxide Nanoparticles

Copper oxide is an example of p-type semiconductor. Adsorptive characteristic of copper surface creates electron hole pair that increases resistance of copper oxide. Detection of redox gases through surface sensitive metal oxides is due to the adsorption of charged surface oxygen species. Increase in resistivity of gas sensors is due to the pre-adsorbed oxygen species of reducing gases. While atoms of injecting gas land on copper surface then charge states exchange electron lone pairs, prompting sensitivity of copper for distinguishing oxidizing & reducing gases depends on alternation for electron lone pairs [104].

The response towards ammonia gas revealed chemical to electrical transduction elements among gas molecules & copper oxide that is regulated through adsorbed oxygen at the surface of metal oxide. By utilizing discharged electrons drive to a rise in resistance of copper oxide on disclose to ammonium gas due to p-type characteristics of metal oxide. Three ends of individual nanoparticles are utilized. Firstly, change in resistance occurs through analyte due to the arrangement of depleted region. Then detection is triggered by particle retained oxygen atom & metal oxide. Finally, concentration of tested analysis is basically below absolute oxygen species on surface [105].

The sensor response for introduction to 1 ppm-5 ppm of $NH_3$ is examined and schematically represented in Figure.5.9 (a) for pure & Cu doped $Co_3O_4$ nanoparticles. From the findings it is clear that surface chemistry unique in all metal oxides but response modulation depends on diameter below 100 nm. Metal oxide is accepted as surface oxygen species release of electrons from copper oxide decreasing resistance by the creation of holes in material on exposing $NH_3$ [106].

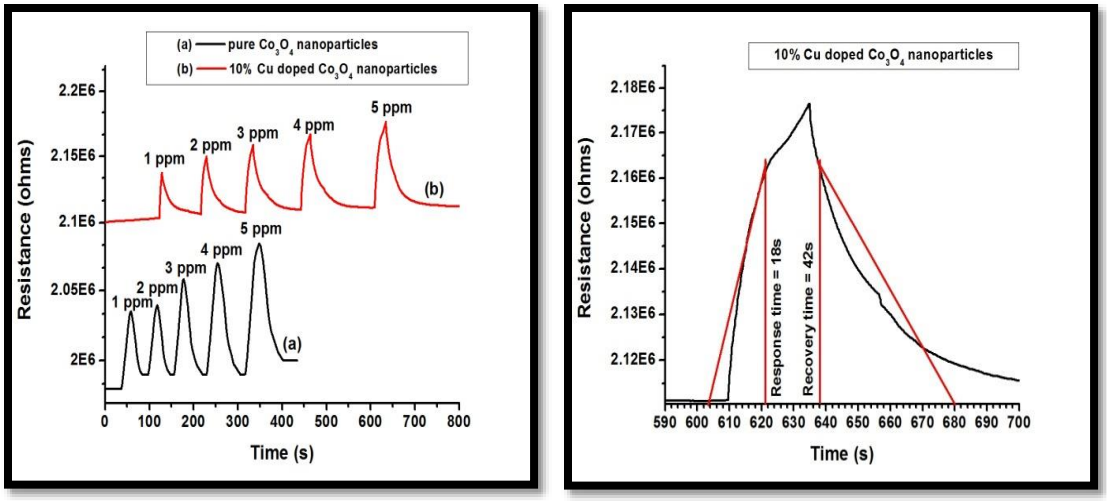


**Figure. 5.9 (a). Sensitivity of pure and Cu doped $Co_3O_4$ nanoparticles at room temperature for different gas concentration and (b) Response and recovery times for 5 ppm of $NH_3$**

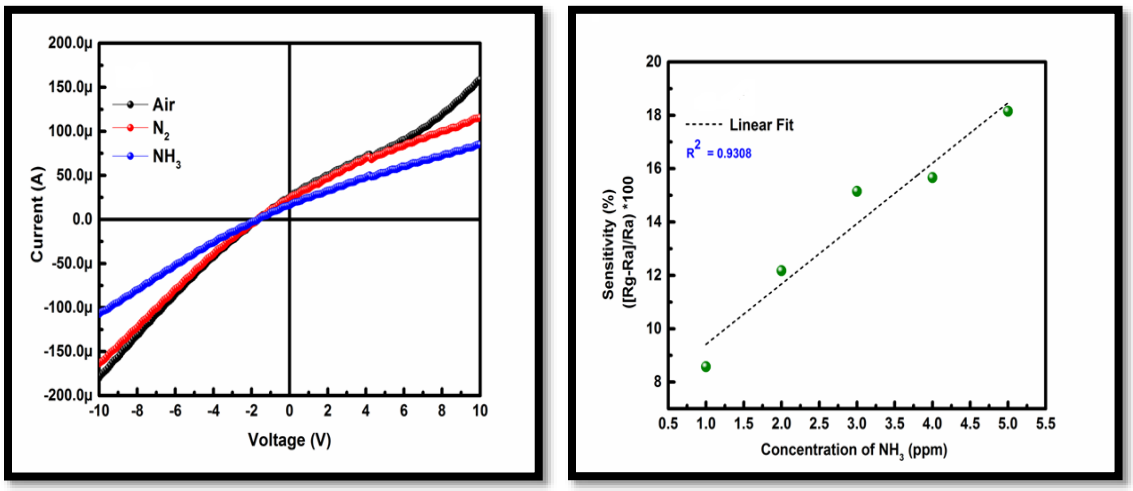


**Figure. 5.9 (c) I-V characteristics and (d) Sensor response linear fit plot of Cu doped $Co_3O_4$ nanoparticles to $NH_3$ (1-5 ppm) gas at room temperature**

When ammonia gas is inserted, resistance increases abruptly & constant at specific concentration then falls after withdrawl of $NH_3$. It is repeated by different gas concentrations like 1 ppm, 2 ppm, 3 ppm, 4 ppm & 5 ppm. Cu doped $Co_3O_4$ prepared nanoparticles exhibit higher & constant reaction towards various concentrations (1ppm-5ppm) of $NH_3$ gas at room temperature. In Fig. 5.9(a) Response of 10% copper doped $Co_3O_4$ nanoparticles sensor is shown. In Fig. 5.9(b) the response & recovery times for the sensor at room temperature towards the 5ppm concentration is shown. The plot representing sensitivity for the sensor towards 5 ppm concentration at different temperatures exhibits the higher sensitivity having response value of 18.1 & lowest response value of 9.5 for the concentration of 1ppm. The sensor had response & recovery times of 18 & 42 seconds respectively at room temperature. The I-V characteristics peak is shown in Fig. 5.9 (c). Sensor response value increased linearly on increasing the $NH_3$ concentration (1-5 ppm) with a regression co-efficient ($R^2$) of 0.9 308 is shown in Fig. 5.9 (d) due to various active sites.

Here, sensor response to $NH_3$ was examined for pure & Cu doped $Co_3O_4$ nanoparticles. Highest sensitivity is shown by sensor having Cu doped $Co_3O_4$ for 5 ppm of $NH_3$ gas. $Co_3O_4$ is doped by copper that changed detecting conduct. Anyway, the sensitivity increases with increase in Cu dopants having 5ppm was efficient than pure $Co_3O_4$ sensor [107].

### 5.20. Gas Sensing Properties of Ni doped Cobalt oxide Nanoparticles

Numerous techniques are utilized for preparing NiO powders in nanometers. Electrical conductivity of NiO nanoparticles is altered by varying Ni vacancies & interstitial oxygen in NiO structure [108, 109]. Increased oxygen adsorption in materials is due to low stability of multivalent transition metal oxides. Facility of enhancing adsorption of oxygen on to NiO is due to the charge compensation by oxidation of Ni ions. Low stability of oxides in redox reactions due to variable oxidation states is by large amount of oxygen adsorbtion in p-type transition metal oxides. Change in the properties of NiO is by the non stoichiometric effect are used in solar cells [110, 111], electrochromic applications [112–115] & optoelectronic applications on the basis of p-n junctions like UV detectors & LEDs [116, 117].

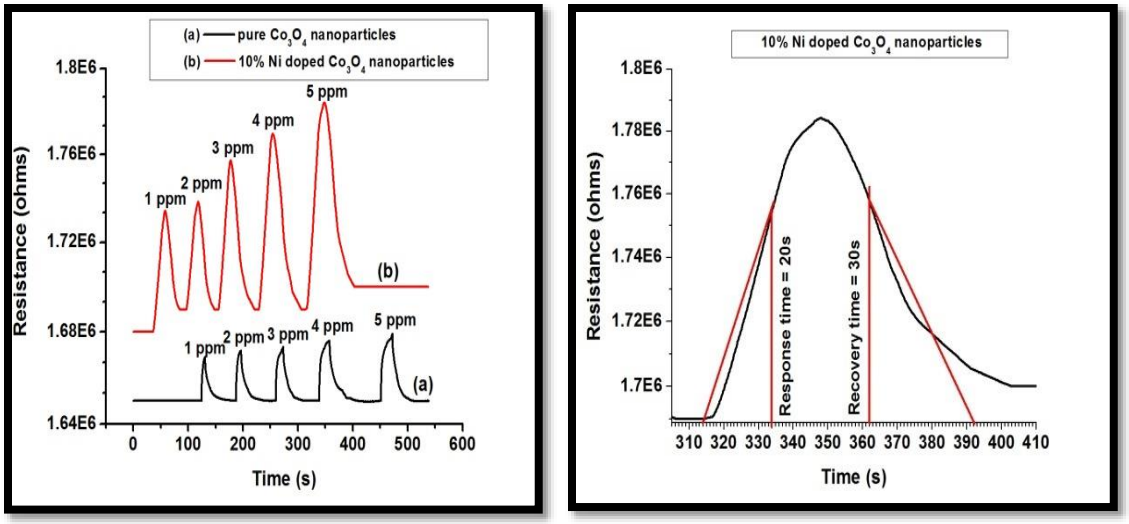


**Figure: 5.10 (a) Sensitivity of pure and Ni doped $Co_3O_4$ nanoparticles at room temperature towards different gas concentrations and (b) response and recovery times towards 5 ppm of $NH_3$**

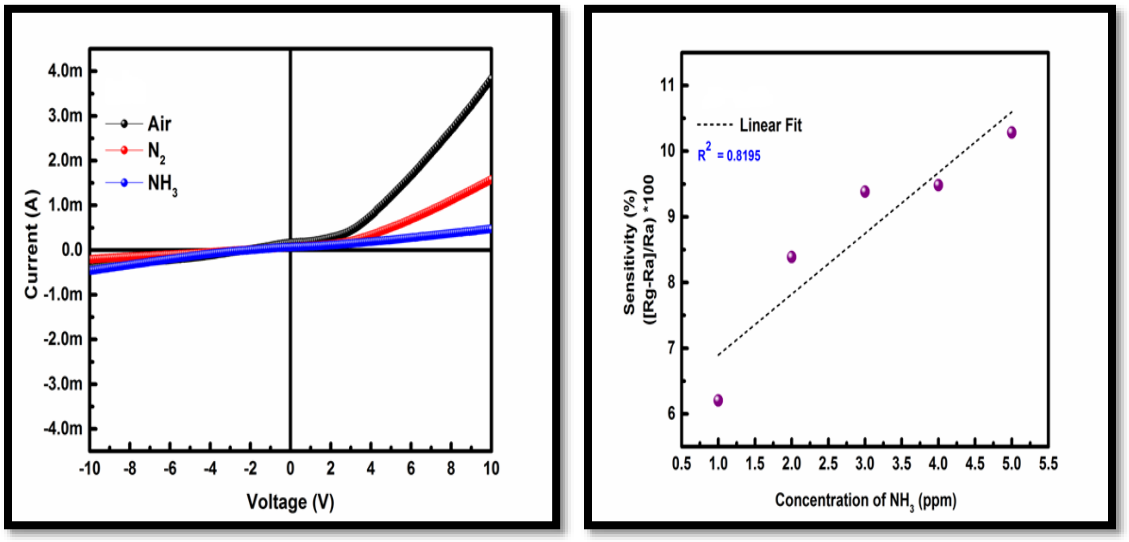


**Figure: 5.10 (c) I-V characteristics and (d) Sensor response linear fit plot of Ni doped $Co_3O_4$ nanoparticles to $NH_3$ (1-5 ppm) gas at room temperature**

In industries NiO had attained great attention due to promising applications in thermistors, fuel cell electrodes, high-power ultra capacitors & optical switching devices. NiO is a proto-p type with wide band gap (3.6-4.0 eV) semiconductor. When compare to their bulk properties NiO instigate breakthroughs in their traditional applications. Chemical composition & chemisorbed oxygen species on sensing surface is the reason for sensor performance [118].

Recently, researchers targeted on hydrothermal process, an easy way of attaining different morphologies of NiO nanoparticles. Formation of NiO nanoparticles involves growth, & oriented attachment processes. Nucleation rate accelerates growth process. Resistance of NiO accelerates while ammonia gas is injected to measurement system because interaction between ammonia & adsorbed oxygen on NiO surface creates $H_2O$ & free electrons. Majority charge carriers in NiO are holes & they recombine with free electrons. Resistance increases due to decrease in number of holes.

In Fig. 5.10 (a), sensitivity of sensor at room temperature towards the concentration of 5 ppm is shown. Resistance of the sensor is due to the creation of holes which fits the observed sensor response. Better response & dynamic range can be utilized in “caution” detection of $NH_3$ provides warning signals [119]. Additionally, sensing response of NiO is dependent on surface morphology, crystallite size, surface states & adsorption efficiency due to specific gas molecules on surface reaction by adsorbed oxygen [120]. Procedure of rapid electron trapping produces higher stablility signal at lower $NH_3$ concentration.

Response & recovery times are 20 seconds & 30 seconds for concentration of 5 ppm (Fig. 5.10 (b)). Sensitivity is examined at minimum detectable concentration of 1 ppm with a response of 6.8 and maximum concentration of 5 ppm by a response of 10.3. I-V analysis shows that the conductivity of the material changes by increase in the channel resistance. I-V curve is shown in Fig.5.10 (c). Linearity of sensor towards various concentrations on that temperature is shown in Fig. 5.10 (d). The linear fit measurements were performed and the regression coefficient $R^2$ was found to be 0.8195.

### 5.21. Summary of the Results

Oxygen an important energetic aspects in air & quantity of oxygen in air is about 20.9% with the aid of volume. Metallic oxides were frequently selfpassivated in opposition to oxygen because constantly oxygen adsorbed on metallic oxide surface while surface is uncovered to air. Oxygen molecules bound to vacancies on metallic oxide surface, capture electrons from surface of metallic oxide & continue to be tightly hold as charged oxygen anion. Captured electrons are then unavailable for conductivity in solid, hence growing the resistance of oxide surface.

In p-type semiconductor, introduction of a depletion layer directs to improve surface conductance [121]. Electron depleted region additionally referred to as space charge layer, a region of excessive resistance & core area of particles there electron densities were less, and a vicinity of tremendously excessive resistance. Thickness of surface charge layer (L) & height of surface conceivable barrier is decided by, (a) surface charge that relies upon quantity of adsorbed oxygen and (b) Debye length that is attribute of semiconductor utilized.

Reducing gases reacts by ionosorbed oxygen at surface releasing electrons which returns to bands. Its, impact is a decline in band bending of surface conductance. In return oxidizing gas would eliminate electrons inflicting furthermore develop in band bending & in n-type semiconductor minimize of surface conductance. P-type semiconductors were featured through presence of free holes in conduction band because of lattice defects like oxygen vacancies, delivered at preparation of material.

While p-type semiconductor metallic oxide is uncovered to air, oxygen molecules get adsorbed on surface of particles & it creates $O2^{-}$ & $O^{-}$ ions through traping electrons from conduction band that creates electron-depleted space-charge layer in surface area. When measurements of nanoparticles are sufficiently decreased it can fully depleted then enhances response to gases. Characteristics of electron dislocate in polycrystalline layers highly rely on grain boundaries [122] that comprise a excessive density of surface state. Those states entice free carriers to create obstacles or highly deplete grains of free carriers & decide material conductivity. Tiny particles had higher density for defects that should have negative impact on transport features [123]. However, transport of electrons

that is decided by microstructure of sensing aspect like grain size of semiconductor particles, additionally decides material's shape and performs a critical position in $NH_3$ gas response.

Better way for ascribing conduction procedure is to think about free charge carriers should overtake inter granular boundaries of peak created by means of band bending at adjoining surfaces of neighboring grains. Barrier heights of surface states may changes through adsorption of molecules from gaseous phase. However, change in conductance (G) at stable temperature is ascribed to variations in surface conductance $G_S$ [124]. Sensor component comprises semiconductor nanoparticles. Microstructure & morphology of those granules were viewed as essential for transducer function. Every particles are linked by their neighbors by grain-boundary contacts. In case of grain-boundary contacts, electrons ought to go throughout the surface potential barrier at every boundary. Variation of barrier peak made electric resistance of component established on gaseous ecosystem [125]. Resistance & gas sensitivity is not essentially established on particle size. In necks, electron switch between particles takes via a channel that is created in space-charge layer at every neck. Width of channel is decided by neck measurement & thickness of surface charge layer (L) & variation by gases offers upward push to gas-dependent resistance of element [126]. Gas sensitivity depends on particle size. Those two models, even though conceptual, point out the significance of microstructure for transducer feature of element. The consequences point out that for a crystallite size larger than 30 nm conduction is underneath grain boundary control.

Interplay among metallic oxide & adsorbed gas is a dynamic process. While a material is uncovered to test gas in air, adsorption & desorption procedures manifest simultaneously. In response procedure adsorption overcomes desorption method till stationary prerequisites were achieved. Here, various adsorbed gaseous molecules equate a wide variety of desorbed ones & electrical conductivity achieves a steady value. When test gas cut off, desorption induces on re-adsorption technique & conductivity reverses to its authentic value. Here, process of conduction is managed with the aid of electron flow via large sequence of inter granular factor contacts. At such contacts a surface barrier creates in presence of surface states that relies upon each chemical reaction by detecting gases & on physical intrinsic traits of the material. Conductivity is an activated process,

considering those electrons having adequate strength to go the barrier take section in electrical conductance. Chemoresistivity is the foundation of sensing mechanism for metallic oxides that composed, of variant of inter granular barrier having subsequent conductivity amendment like response to surface chemical reactions with environmental gases. When barrier modulation takes place at surface, bulk doesn't longer take section in the complete procedure of sensing, & an excessive surface to volume ratio is wanted to enlarge gas response.

Sensing process is a surface-controlled kind & gas sensitivity is associated to thickness of active layer, grain size, surface state, oxygen adsorption quantity, active energy of oxygen adsorption & lattice defects [127, 128]. Annealing at high temperature enhances resistivity because chemisorption of oxygen at grain boundaries that drives to creation of extrinsic capture states localized at grain boundaries. Crystal orientation, grain boundaries & film thickness depends on density of captured states created because of chemisorbed oxygen. Those states trapped free electrons from bulk of grains to form potential barrier through depletion in region adjacent to grain boundaries. Those potential barriers reduce motion of carriers by enhancing resistivity [129].

Atmospheric oxygen molecules were adsorbed on surface sites & ionized by having an electron from the conduction band & as a consequence ionosorbed on surface like $O_{(ads)}$ [130]. Electron dislocation among adsorbed oxygen molecules & semiconductor surface consequences in creation of depletion layer additionally recognized as space charge layer. Space-charge layer is a location having poorcarriers because of electron trapping with the aid of chemisorbed oxygen. Such electron transfer & succeeding advent of electron depleted vicinity due to reduction in conductance of sensor material. However, electrical conductivity relies upon highly on surface states formed through molecular adsorption which effects in space charge layer adjustments & band modulation. Impact of adsorbed oxygen, numerous types of adsorbed oxygen, band bending related by oxygen & gas adsorption, temperature based adsorption and desorption method additionally act a role.

Examining crystallite size, D (pure $Co_3O_4$ = 47.75nm, Zn = 45.17nm, Fe = 44.49nm, Cu = 48.42nm, Ni = 49.53nm) of samples electrical conduction is considered to underneath grain boundary manipulate regime. $NH_3$ is a reducing gas that receives chemisorbed at surface of CoO grains & capture electrons at surface. Electrons taken from ionized donors through conduction band & density of majority charge carriers at gas-solid interface is decreased. It directs to creation of surface barrier for electrons. By expand of oxygen ions density on surface, similarly oxygen adsorption is hindered. Consequently, at junctions among CoO grains, depletion layer & potential barrier guide to rise in electrical resistivity value. These values are highly based on attention of adsorbed oxygen ions of surface. Adsorption of atmospheric oxygen drives to a band bending.

Producing n-type & p-type dopants in $NH_3$ gas sensor may alternate the number of these adsorbed oxygen ions & enhances resistance. Response in existence of $NH_3$ reducing gas headed to consuming electrons & similarly expands surface barrier height & therefore resistance of sensor. Adsorption of $NH_3$ gas would in addition develop band bending. Electrons fed on these reactions were withdrawn from conduction band, as a result elevating resistivity of material. Dopants in metallic oxide substances generally have an effect on structural & electrical properties. Dopant factors regularly separate to grain boundaries in crystalline metallic oxide & limit the grain growth in succeeding annealing. Electrically, dopants create ionic & digital defects. Such defects have an effect on role of Fermi energy level in return is predicted to have an effect on gas sensitivity of semiconducting oxides.

It is nicely recognized that gas sensing mechanism in oxide primarily based substances is surface regulated, whereby grain size, surface states & oxygen adsorption play a huge role. Large surface area normally affords much adsorption-desorption sites & as a result increased sensitivity [131, 132]. Atmospheric oxygen adsorbed on sensor surface & relying on temperature of operation, various oxygen species are formed on surface. While sensor is uncovered to reducing gas, it interacts by oxygen species chemisorbed on semiconductor surface & emits electrons to conduction band. It reduces in the quantity of surface $O^-$ & $O2^-$ ions, directs to enhance in number of electrons in conduction band. It subsequently enhances conductivity & therefore sensitivity of those metallic oxide sensors [133].

Sensitivity of metallic oxide gas sensors notably relies upon temperature. It is recognized that response among metallic oxide & adsorbed gas is a dynamic & reversible method & each kinetics & equilibrium rely on temperature. However, gas response usually relies upon accessibility of reducing gases & O-2 (ads) species. Recreation of conductance occurs on elimination of $NH_3$ & existence of ambient oxygen. Reducing gas ($NH_3$) donates electrons to CoO. However, resistance of sensor reduces or conductance enhances. Additionally to surface reaction by adsorbed oxygen species, chemical conversion is other feasible reaction process that affects conductivity of sensor. Chemical conversion of gas sensing substances by direct reaction with target gas is recognized as a necessary mechanism which alters conductivity & creates an excessive sensitivity in various sensing substances of metallic oxides.

**5.22. Conclusion**

The present work has been carried out to study the gas sensing properties of Zn doped $Co_3O_4$ nanoparticles synthesized by the hydrothermal method. The newly prepared Fe doped $Co_3O_4$ nanoparticles revealed a higher & stable response to $NH_3$ gas (1 ppm-5 ppm) at room temperature. The decrease in sensitivity of materials (Zn, Cu and Ni) other than Fe doped $Co_3O_4$ nanoparticles is attributed to enhance in free electron concentration &variation in resistance happened due to gas adsorption low in comparison to improved carrier concentration. Anyway, sensitivity response reduces at higher temperatures, due to desorption of oxygen adsorbates from surface of sensor. Carrier concentration enhanced by intrinsic thermal excitation & reduced Debye length. It will lead to reduced gas response at higher temperatures. Response values of $NH_3$ were associated with particular surface area & pore size of sensor material. Recently synthesized Fe doped $Co_3O_4$ nanoparticles are potential gas sensing materials, specifically for $NH_3$ sensing applications.

## References


[1] Mane, S. Kulkarni, S. Navale, A. Ghanwat, et.al, Ceram. Int. 40 (2014) 16495–16502.

[2] G. C. Franco, A. T. Silver, J. M. Domínguez, A. S. Juárez Thin Solid Films (2000) 373, 141.

[3] S. C. Gadkari, K. Manmeet, V. R. Katti, V. B. Bhandarkar, K.P. Muthe, S. K. Gupta Encyclopedia of sensors, American Scientific Publishers (2006).

[4] D. S. Lee, H. Y. Jung, J. W. Lim, M. Lee, S. W. Ban, et. al, Sens. and Actu. (2000) 71, 90.

[5] A. Hulanicki, S. Geab and F. Ingman Pure and Appl. Chem. (1991) 63, 1247.

[6] J. Stetter and W. Penrose Sensors update (2002) 10, 189.

[7] A. Hulnnicki, S. Clab, ind K Ingm.in, Pure & Appl. Chcm. 63, 1247 (1991).

[8] G. Sberveglieri, R. Murri and P. Nicola Sensors and Actuators B (1995) 23, 177.

[9] M. Andersson, M. Holmberg, I. Lundström, A. Lloyd-Spetz, P. Mårtensson, R. Paolesse, C. Falconi, E. Proietti, C. Di Natale and A. D'Amico Sensors and Actuators B (2001) 77, 567.

[10] S. J. Jung and H. Yanagida Sensors and Actuators B (1996) 37, 55.

[11] S. Nakagomi, K. Okuda and Y. Kokubun Sensors and Actuators B (2003) 96, 364.

[12] S. Jonda, M. Fleischer and H. Meixner Sensors and Actuators B (1996) 34, 396.

[13] Criindler, "Chemical Sensors: An Introduction for Scientists and Kngineers." Springer, Berlin, 2007.

[14] Y. Shimizu and M. Egashira MRS Bulletin (1999) 24, 18.

[15] C. Xu, T. Jun, N. Miura and N. Yamazoe Chemical Letters (1990) 3, 441.

[16] G. G. Mandyo, E. Castaño, F. J. Gracia, A. Cirera, et.al, Sens. and Actu. B (2003) 95, 90.

[17] C. O. Park and S. A. Akbar, J. Mater.Sci (2003) 38, 4611.

[18] Korotcenkova, G.; Cho, B.K. Sens. Actuators B 2011, 156, 527–538.

[19] W. H. Brnttain and J. Bardeen, Hell. Si/sf. Tech. J. 32, 1 (1953).

[20] T. Seiyama, A. Kato, K. Fujiishi, and M. Nagatani, Anal. Chem. 34, 1502 (1962).

[21] N. Yamazoe and N. Miura, "Chemical Sensor Technology" (S. Yamauchi, Ed.), Vol. 4, p. 19. Kodansha, Tokyo, 1992.

[22] H. Meixner and U. Lampe, Sens. Actuators, B 33, 198 (1996).

[23] V. E. Bochenkov and G. B. Sergeev, Adv. Coll. Int. Sci. 116, 245 (2005).

[24] L. Fu, L≫Cao, Yu. Liu, and D. Zhu, Adv. Coll Int. Sci. 111, 133 (2004).

[25] V. E. Bochenkov and G. B. Sergeev, Russ. Chcm. Rev. 7b, 1013 (2007).

[26] G. Jimenez-Cadena, J. Riu, and K X. Rius, The Analyst 132, 1083 (2007).

[27] Seong-Yong Jeong, Jun-Sik Kim, Jong-Heun Lee, Advanced Materials, 2020, 30, 202075.

[28] V. R. Katti, M. Kaur, K. P. Muthu, V. B. Bhandarkar, S. C. Gadkari and S. K. Gupta DAE Solid Stae Physics Symposium (2003) 46, 441.

[29] N. Yamazoe, J. Tamaki and N. Miura Materials Sci. Engg. (1996) 41, 178.

[30] V. B. Bhandarkar, V. R. Katti, M. Kaur, S. C. Gadkari, Asian J. Phys. (2005) 9, 1.

[31] M. Stankova, X. Vilanova, E. Llobet, J. Calderer, et. al, Sens. and Actu. B (2005) 105, 271.

[32] L. Tommie. Jr. Royster, D. Chatterjee, et. al, Sens. and Actu. B (1998) 53, 155.

[33] W. Qu and W. Wlodarski Sensors and Actuators B (2000) 64, 42.

[34] Y. S. Kim, S. C. Ha, K. Kim, H. Yang, S. Y. Choi, Y. T. Kim, J. T. Park, C. H. Lee, J. Choi, J. Paek and K. Lee Appl. Phys. Lett. (2005) 86, 213105.

[35] L. G. Teoh, I. M. Hung, J. Shieh, W. H. Lai, et. al, Electrochem. Solid State Lett. (2003) 6, G108.

[36] M. Bendahan, R. Boulmani, J. L. Seguin, K. Aguir, Sens. and Actuators B (2004) 100, 320.

[37] J. Tamaki, A. Hayashi, Y. Yamamoto and M. Matsuoka, Sens. and Actu. B (2003) 95, 111.

[38] J. Liu, X. Wang, Q. Peng and Y. Li, Sensors and Actuators B (2006) 115, 481.

[39] C Xu, J. Tamaki, N. Miura, and N. Yamazoe, Sens. Actuators, B 3, 147 (1991).

[40] R. C. Aiyer, S. G. Ansari, P. Boroojerdian, R. N. Karekar, S. K. Kulkarni, and S. R. Sainkar, Thin Solid Films 295, 271 (1997).

[41] A. Gurlo, M. Ivanovskaya, N. Barsan, M. Scweizer-Berberich, U. Weimar, W. Gopel, and Л. Dieguez, Sena. Actuators, B 44, 327 (1997).

[42] O. K. Tan, W. Zhu, Q. Yan, and L. B. Kong, Sena. Actuators, B 65, 361 (2000).

[43] C. R. Michel, E. Lopez-Mena, and A. H. Martinez, Talanla 74, 235 (2007).

[44] Y. Shimizu, T. Hyodo, and M. Egashira, /. Eur. Cer. Soc. 24, 1389 (2004).

[45] U. Egashira, Y. Shimizu, et. al, Mater. Res. Soc. Symp. Proc, 2005, Vol. 828, p. A 1.1.1.

[46] V. R. Shinde, T. P. Gujar, and C D" Lokhande, Sens. Actuators, B 123, 701 (2007).

[47] H. Xu, X. Liu, D. Cui, M. Li, and M. Jiang, Sens. Actuators, H 114, 301 (2006).

[48] Y. Shen, T. Yamazaki, Z. Liu, C Jin, T. Kikuta, et.al, Thin Solid Films 516, 5111 (2008).

[49] M. Iwamoto, "Chemical Sensor Technology" (S. Yamauchi, Ed.), Vol. 4, p. 63. Kodansha, Tokyo, 1992.

[50] S. Wlodek, K. Golbow, and F. Consadori, Sens. Actuators, li 3, 123 (1991).

[51] W. M. Sears, K. Colbovv, and F. Consadori, Sens. Actuators, B 19, 333 (1989).

[52] I. Simon, N. Barsan, M. Bauer, and U. Weimar, Sens. Actuators. B 73, I (2001).

[53] D. K. Aswal and S. K. Gupta Science and Technology of Chemiresistor Gas sensors Nova Science Publishers (2007) India.

[54] F. Cosandey, G. Skandan, A. Singhal, JOM-e (2000) 52, 10.

[55] Cerdà, J.; Cirere, A.; Vilà, A.; Cornet, A.; et.al, Thin Solid Films 2001, 391, 265–269.

[56] Brezmes, J.; Llobet, E.; Vilanova, X. et. al, Sens. Actuat. B-Chem. 2000, 69, 223–229.

[57] Y. K. Chung. M. H. Kim, W. S. Um, H. S. Lee, J. K. Song, S. C. Choi, K. M. Yi, M. J. Lee and K. W. Chung Sensors and Actuators B (1999) 60, 49.

[58] G. S. D. Evi, S. Manorama, V. J. Rao Sensors and Actuators B (1995) 28, 31.

[59] H. Liu, S. P. Gong, Y. X. Hu, J. Q. Liu, D. X. Zhou Sens. and Actuators B (2009) 140, 190.

[60] Y. Yamada and M. Ogita Sensors and Actuators B (2003) 93, 546.

[61] S. H. Wang, T. C. Chou and C. C. Liu Sensors and Actuators B (2003) 94, 343.

[62] D.V. Ponnuvelu et al, Applied Surface Science. 2015 (355) 726–735.

[63] R. Li, L. Wang, D. Kong, L. Yin, Bioact. Mater. 2018, 3, 322–333.

[64] Tian-tian Li, Na Bao, et al, R. Soc. open sci. 2018, 5, 171788.

[65] Prabakaran Shankar, John Bosco Balaguru Rayappan, Sci. Lett. J. 2015, 4, 126.

[66] Pisarev RV, Pavlov V V, et al, Phys. Rev. B. 2010, 82, 224502.

[67] Ray P, Jeon S H, et al, RSC Adv. 2014, 4, 23604-23609.

[68] Yamazoe N, Sakai G, et al, Catal. Surv.Asia.2003, 7, 63-75.

[69] Morrison SR, Sens. Actuate, 1987, 12, 425- 440.

[70] Iwamoto M, Yoda Y et al J. Phys. Chem. 1978, 82, 2564-2570

[71] Hu Z, Xu M, et al, J. Mater. Chem. A. 2015, 3, 14046-14053.

[72] Chen Y, Shen Z R, et al, RSC Adv. 2015, 6, 2504-2511.

[73] Zhenyu Yuan, Rui Li, et al, Sensors. 2019, 7, 1495.

[74] Srinivasulu Kanaparthi, Shiv Govind Singh, Mat.Sci. for Energy Tech. 2020, 3, 91- 96.

[75] L.L. Wang, R. Zhang, T.T. Zhou, et al, Sens. Actuators B. 2016, 223, 311–317.

[76] L.L. Wang, W.B. Ng, J.A.N.J. Jackman. Cho, Adv. Funct. Mater. 2016, 26, 2097–2103.

[77] H.P. Uskaikar, N.P. Shetti, et al, Mater. Today Proc. 2019, 18, 963–967.

[78] A.B. Bandi, N.P. Shetti, S.J. Malode, et al, Mater. Today Proc. 2019, 18, 590–595.

[79] S.D. Bukkitgar, N.P. Shetti, R.M. Kulkarni, Sens. Actu. B Chem. 2018, 255, 1462–1470.

[80] S. D. Bukkitgar, N. P. Shetti, et al, J. Electrochem. Soc. 2019, 166, 3072-3078.

[81] B. Wu et al. Microporous and Mesoporous Materials. 2016, 225, 154-163.

[82] N. P. Shetti, S.D. Bukkitgar, K.R. Reddy, et al, Biosens.Bioelectron. 2019, 141, 111417.

[83] R. Li, L. Wang, D. Kong, L. Yin, Bioact. Mater. 2018, 3, 322–333.

[84] J. Deng et al. Sensors and Actuators B. 2015, 209, 449–455.

[85] J. Li, S. Sathasivam, A. Taylor, C.J. Carmalt, I.P. Parkin, RSC Adv. 2018, 8, 42300– 42307.

[86] R. Vittal, K.-C. Ho, Renew. Sustain. Energy Rev. 2017, 70, 920–935.

[87] J.M. Choi, J.H. Byun, S.S. Kim, Sens. Actuators B. 2016, 227, 149–156.

[88] D.V. Ponnuvelu et al, Applied Surface Science. 2015, 355, 726–735.

[89] Y.C. Liang, W.K. Liao, X.S. Deng, J. Alloys Comp. 2014, 599, 87–92.

[90] C.W. Na, H.S. Woo, I.D. Kim, J.H. Lee, Chem. Commun. 2011, 47, 5148–5150.

[91] J.R. Huang, Y.J. Dai, C.P. Gu, Y.F. Sun, J.H. Liu, J. Alloys Comp. 2013, 575, 115–122.

[92] J.M. Xu et al. Journal of Alloys and Compounds. 2015, 619, 361–367.

[93] N. Singh, C. Yan, and P. S. Lee, Sensors and Actuators, B, vol. 150, no. 1, pp. 19–24, 2010.

[94] Jian-Wen Wang and Yi-Ming Kuo Journal of Nanomaterials. 2013.

[95] Eranna G, Joshia BC, Runthalaa DP, Gupta RP (2014) Oxide materials for development of integrated gas sensors - A comprehensive review. Crit Rev Solid State Mater Sci 29: 111-188.

[96] Wang C, Yin L, Zhang L, Xiang D, Gao R (2010) Metal Oxide Gas Sensors: Sensitivity and Influencing Factors. Sensors 10: 2088-2106.

[97] Hoa ND (2012) One-dimensional Semiconducting Metal Oxides: Synthesis, Characterization and Gas Sensors Application. Chapter 2, in Intelligent Nanomaterials: Processes, Properties, and Applications, Eds: A. Tiwari, A. K. Mishra, H. Kobayashi, A. P. F. Turner, Scrivener Publishing LLC. View

[98] Traversa E, Schäf O, Di Bartolomeo E, Knauth P (2002) Nanocrystalline oxides for gas sensing, In Nanocrystalline Metals and Oxides, Selected Properties and Applications. Kluwer Academic Publishers 189-234. View

[99] Varghese OK, Grimes CA (2004) Metal Oxide Nanostructures as Gas Sensors, In Encyclopedia of Nanoscience and Nanotechnology. Ed. H.S. Nalwa 5: 505-521.

[100] Korotcenkov G (2013) Handbook of Gas Sensor Materials, Properties, Advantages and Shortcomings for Applications, Vol. 1: Conventional Approaches, Integrated Analytical Systems Series, Ed.: Radislav A. Potyrailo, Springer.

[101] Korotcenkov G (2013) Handbook of Gas Sensor Materials: Properties, Advantages and Shortcomings for Applications, Vol. 2: New Trends and Technologies (Integrated Analytical Systems), Springer.

[102] R. B. King (Ed.) (2005) Encyclopedia of Inorganic Chemistry, 10 Volume set, 2nd Ed., ISBN 978-0-470-86078-6.

[103] Yamazoe N, Kurokawa Y, Seiyama T (1983) Effects of additives on semiconductor gas sensors. Sens. Actuators 4: 283-289.

[104] Prabakaran Shankar, John Bosco Balaguru Rayappan, Sci. Lett. J. 2015 (4) 126.

[105] J. Li, S. Sathasivam, A. Taylor, C.J. Carmalt, et al, RSC Adv. 2018 (8) 42300–42307.

[106] Bedi R. K and Singh I, ACS Applied Materials & Interfaces. 2010 (2) 1361-1368.

[107] D. Sivalingam, J. B. B Rayappan, et. al, Int. J. Nanosci. 2011 (10) 1161.

[108] Y.-M. Lee, C.-H. Hsu, H.-W. Chen, Appl. Surf. Sci. 255(8), 4658– 4663 (2009)

[109] S. Kim, D. Chul, H. Lee, J. Appl. Phys. 112, 3 (2012)

[110] X. Xu, Z. Liu, Z. Zuo, M. Zhang, Z. Zhao, et. al, Nano Lett. 15(4), 2402–2408 (2015)

[111] J. He, H. Lindström, A. Hagfeldt, et. al, J. Phys. Chem. B 103(42), 8940–8943 (1999)

[112] H. Moulki, C. Faure, M. Mihelcic, A.S. Vuk, F. Svegl, B. Orel, G. Campet, M. Alfredsson, A.V. Chadwick, D. Gianolio, A. Rougier, Thin Solid Films 553, 63–66 (2014)

[113] D.R. Sahu, T. Wu, S. Wang, J. Huang, J. Sci. Adv. Mater. Devices 2(2), 225–232 (2017)

[114] S. Pereira, A. Goncalves, N. Correia, J. Pinto, L. Pereira, R. Martins, E. Fortunato, Sol Energy Mater. Sol Cells 120, 109–115 (2014)

[115] G.F. Cai, C.D. Gu, J. Zhang, P.C. Liu, X.L. Wang, Y.H. You, J.P. Tu, Electrochim. Acta 87, 341–347 (2013)

[116] A. Echresh, C.O. Chey, M. Zargar Shoushtari, V. Khranovskyy, O. Nur, M. Willander, J. Alloys Compd. 632, 165–171 (2015)

[117] H. Wang, Y. Zhao, C. Wu, G. Wu, Y. Ma, X. Dong, B. Zhang, G. Du, Opt. Commun. 395–397, 94 (2017).

[118] C. Wang, X. Cui, J. Liu, X. Zhou, X. Cheng, P. Xiaolong, S. Xiaowei, H. Li, J. Zheng, G. Lu, ACS Sens. 1(2), 131–136 (2016).

[119] M. M. Gomaa, G. RezaYazdi, M. Rodner, G. Greczynski, M. Boshta, et. al, Journal of Materials Science: Materials in Electronics (2018) 29:11870–11877

[120] C.S. Rout, M. Hegde, A. Govindaraj, Nanotechnology 18, 20 (2007)

[121] G. Heiland Sensors and Actuators (1982) 2, 343.

[122] M. Ahsan, T. Tesfamichael, M.Ionescu, et. al, Sens. and Actuators B (2011) 162, 14.

[123] I. Karkkanen, M. Kodu, T. Avarmaa, J. Kozlova, L. Matisen, H. Mandar, A. Saar, V. Sammelselg and R.Jaaniso, Procedia Engineering, (2010) 5, 160.

[124] N. Bârsan and U. Weimar J. Phys. Condens. Matter (2003) 15, R813.

[125] H. Ihokura SnO based inflammable gas sensors, Doctoral Thesis, Kyushu University, 1983, 52.

[126] J. Dayan, S. R. Sainkar, R. N. Karekar, R. C. Aiyer, Thin Solid Films (1998) 325, 254.

[127] A. Rothschild and Y. Komem Journal of Appl. Phys. (2004) 95, 6374.

[128] M. E. Franke, T. J. Koplin and U. Simon Small (2006) 2, 36.

[129] S. Major, A. Banerjee and K. L. Chopra Thin Solid Films (1986) 143, 19.

[130] J. Marc, S. Madau and R. Morrison, Chemical sensing with Solid State Devices, Academic Press New York (1989).

[131] Z. M. Zeng, K. Wang, Z. X. Zhang, J. J. Chen, W. L. Zhou, Nanotech. (2009) 20, 045503.

[132] V. D. Kapse, S. A. Ghosh, G. N. Chaudhari, F. C. Raghuwanshi, Talanta (2008) 76, 610.

[133] V. D. Kapse, S. A. Ghosh, F. C. Raghuwanshi, et. al, Sens. and Actu. B (2009) 137, 681.